Cureus Journal of Computer Science
https://doi.org/10.7759/s44389-026-00375-6

Original Article

Gabor-Enhanced EfficientNet for Automated Bone Cancer Classification in Pelvic Computed Tomography (CT) Images

Paramjit Kour [1, ✉], Vibhakar Mansotra [1]

1. *Computer Science and IT, University of Jammu, Jammu, IND*

Received: September 07, 2026 | Review began: September 10, 2026 | Review ended: November 13, 2026 | Published: November 17, 2026

© **Copyright** 2026
This is an open access article distributed under the terms of the Creative Commons Attribution License CC-BY 4.0., which permits unrestricted use, distribution, and reproduction in any medium, provided the original author and source are credited.

Abstract

Bone cancer classification from computed tomography (CT) images is challenging because abnormal changes in bone structure and texture can be subtle. This study proposes a Gabor-Enhanced EfficientNet model for automated classification of pelvic CT images into Normal and Cancerous categories. The proposed framework first preprocesses the CT images and applies Gabor filtering to enhance directional texture and structural patterns. The Gabor representation is then fused with the original CT image to preserve both anatomical and texture information. The fused images are classified using EfficientNet, which learns discriminative features for binary classification. The effectiveness of the proposed model is evaluated using a comprehensive set of performance indicators, namely accuracy, precision, sensitivity, specificity, F1-score, and Matthews correlation coefficient. The proposed method combines Gabor-based texture features with deep learning for bone cancer classification from CT images.

Categories: Health Informatics, Medical Expert systems, Deep Learning

Keywords: : bone cancer, pelvic ct images, feature fusion, gabor filter, efficientnet., deep learning, gabor filter bank, bone cancer, medical image classification, pelvic ct

Introduction

Medical imaging is essential for identifying and assessing bone abnormalities, as different imaging techniques provide complementary information about tumor-associated structural and pathological changes. Evidence from previous studies indicates that computed tomography (CT) has considerable potential for detecting and staging bone malignancies [1]. CT provides detailed cross-sectional visualization of bone structures, enabling assessment of bone morphology, cortical destruction, mineralization, and tumor involvement [2]. CT is particularly valuable for assessing the structural characteristics and local extent of bone lesions and their relationship with surrounding anatomical structures. However, interpreting CT images can be difficult because malignant and metastatic bone lesions may exhibit subtle and complex features that can resemble those associated with benign lesions, infections, or other skeletal abnormalities [3].

Bone cancer is a rare but clinically significant malignancy characterized by the abnormal and uncontrolled growth of cells within bone tissue. Although primary bone cancer is relatively uncommon, timely and accurate detection is essential because tumor extent, local invasion, and metastatic spread can significantly influence treatment selection and patient prognosis [4]. The complexity and variability of bone lesions may therefore make reliable diagnosis difficult through visual assessment alone. This highlights the need for automated computer-aided diagnostic methods that can assist clinicians in the consistent detection and classification of suspicious bone lesions from CT images.

How to cite this article:
Kour P, Mansotra V (November 17, 2026) Gabor-Enhanced EfficientNet for Automated Bone Cancer Classification in Pelvic Computed Tomography (CT) Images. Cureus J Comput Sci 3 : es44389-026-00375-6. DOI https://doi.org/10.7759/s44389-026-00375-6

The growing application of deep learning in medical image analysis has enabled automated systems to learn complex representations and identify subtle pathological patterns. Among deep learning methods, convolutional neural networks (CNNs) can automatically learn multiple levels of visual information from medical images, ranging from basic patterns such as edges and textures to more complex structural characteristics [5]. This reduces the need for manually designed features and has supported their use in bone tumor imaging applications, including tumor detection, classification, and segmentation [6]. In CT imaging, deep learning models can utilize structural information from cross-sectional scans to distinguish malignant from non-malignant bone abnormalities. However, limited research has focused specifically on bone cancer classification using CT images [7], indicating a need for further investigation in automated CT-based classification.

The present study proposes a Gabor-Enhanced EfficientNet framework for bone cancer classification using pelvic CT images. The proposed framework incorporates CT image preprocessing, Gabor-based feature extraction, deep learning model training, and binary classification into Normal and Cancerous categories. The proposed study makes the following key contributions:

1. Design of an automated deep learning framework for differentiating between Normal and Cancerous pelvic CT images.

2. Incorporation of Gabor-based texture enhancement to emphasize directional, textural, and structural characteristics present in CT images.

3. Integration of the enhanced image representation with EfficientNet to learn informative features and perform binary bone cancer classification.

4. Comprehensive evaluation of the proposed model using six performance measures, supported by graphical analyses such as the receiver operating characteristic (ROC) curve and performance plots, to provide a detailed assessment of its classification performance.

Literature review

This section reviews previous studies that have explored medical imaging and deep learning approaches, particularly those incorporating Gabor filter-based texture analysis, for the detection and classification of different types of cancer.

Deivasigamani et al. [8] presented a CNN-based method for melanoma image classification by incorporating texture information into the learning process. Initially, histogram equalization was used to improve the visual quality and contrast of the input images. Gabor filters were then employed to capture relevant texture patterns from the processed images. These representations were subsequently provided to a CNN classifier for melanoma identification. The reported results indicated that the integration of Gabor-based texture information with CNN contributed to effective classification performance. Cai et al. [9] proposed a renal cancer classification method that fused deep learning features with handcrafted texture descriptors, including Gabor features. The fusion of these complementary features improved the effectiveness of histopathological image classification.

Karim et al. [10] developed a multi-feature approach by extracting color, shape, and texture information using different filters, including Gabor features. These handcrafted features were combined with deep features from three deep learning models, achieving promising classification performance. Attallah [11] proposed SCaLiNG, a computer-aided diagnostic framework designed to support the early detection and classification of skin cancer. The method integrated three lightweight CNNs with Gabor wavelets to capture spatial, textural, and frequency-based features, achieving promising classification performance.

Sarvestani et al. [12] investigated mammogram image classification using image enhancement techniques to improve the visibility of breast tissue microcalcifications. Their approach employed a fuzzy-based region of interest method to highlight relevant areas, along with Gabor filtering for extracting discriminative texture features. The study demonstrated the potential of combining region of interest-based enhancement and Gabor features for mammographic image

How to cite this article:
Kour P, Mansotra V (November 17, 2026) Gabor-Enhanced EfficientNet for Automated Bone Cancer Classification in Pelvic Computed Tomography (CT) Images. Cureus J Comput Sci 3 : es44389-026-00375-6. DOI https://doi.org/10.7759/s44389-026-00375-6

classification. Kour and Mansotra [13] combined CNN-based deep learning with Gabor filtering to develop a bone cancer classification model using MRI images. Their study evaluated the effectiveness of integrating deep features with texture information and reported promising results for bone cancer detection.

Previous studies have established the usefulness of Gabor filters for capturing discriminative texture patterns in medical images. However, the reported performance differs according to the cancer type, imaging modality, dataset, feature extraction strategy, and classification method. Table *1* presents representative Gabor filter-based studies, detailing the cancer type, imaging modality, texture extraction method, classifier, and reported performance. The studies summarized in the table achieved classification accuracies exceeding 90%, demonstrating the potential of Gabor-based texture representation for cancer image analysis.

Recent studies have also increasingly combined Gabor-based texture information with deep learning methods for cancer detection and classification across different medical imaging modalities. Despite these developments, the use of Gabor-based texture analysis with CT images remains comparatively limited. In particular, few studies have examined the combination of Gabor-based texture extraction and deep learning for bone cancer classification. This limited evidence provides the motivation for the present study, which integrates Gabor-based texture information with a deep learning model for bone cancer classification using CT images.

Reference	Gabor-Based Approach	Cancer Type	Classifier	Imaging Modality/Dataset
Bakheet and Al-Hamadi [14]	Optimized Gabor-based entropic features	Melanoma/skin cancer	Multilevel neural network	Dermoscopic images
Al-Kadi [15]	Multiresolution Gabor-filter energy combined with fractal texture feature	Brain tumor (meningioma subtypes)	Classification framework	Histopathology images
Linder et al. [16]	Gabor-filtered texture images for distinguishing tumor epithelium/stroma	Colorectal cancer tissue	SVM-based texture classifier	Histopathology images
Kumar et al. [17]	Modified context-aware multiresolution Gabor filters	Breast cancer	Long short-term memory	Histopathology images
Santiago-Montero et al. [18]	Multi-scale Gabor modeling of lesion texture	Melanoma	Gabor-based descriptor	Dermoscopic images

TABLE 1: Summary of Gabor filter-based approaches for cancer image detection and classification

SVM, Support Vector Machine

How to cite this article:
Kour P, Mansotra V (November 17, 2026) Gabor-Enhanced EfficientNet for Automated Bone Cancer Classification in Pelvic Computed Tomography (CT) Images. Cureus J Comput Sci 3 : es44389-026-00375-6. DOI https://doi.org/10.7759/s44389-026-00375-6

Materials And Methods

Methodology

This section describes the proposed Gabor-Enhanced EfficientNet framework developed for bone cancer classification using pelvic CT images. The framework consists of sequential stages, including image preprocessing, Gabor-based texture extraction, feature fusion, and final classification. The complete workflow of the proposed approach is presented in Figure *1*, while the computational procedure and sequence of operations are summarized in Algorithm 1.

Algorithm 1: Gabor-Enhanced EfficientNet for Pelvic CT for Bone Cancer Classification

Input: Pelvic CT images in JPG/PNG format

Output: Predicted class: Normal or Cancerous

Step 1. Dataset preparation

Let the pelvic CT dataset be $D = (I_i, y_i)i =_N^1$

Where I_i represents the ith CT image, and $y \in \{0, 1\}$, where 0-Normal and 1-Cancerous.

Step 2. Image preprocessing

• Resize each CT image to 224 × 224 pixels.

• Normalize pixel intensities to the range of 0 to 1.

Step 3. Data Splitting

$D = D_{\text{train}}, D_{\text{valid}}, D_{\text{test}}$

Step 4. Gabor Texture Extraction

The Gabor filter is defined as: $G_{\max}(x, y) = \max|G_{(s,\theta)}(x, y)|$

Step 5. Gabor Feature Map

The maximum response from the applied Gabor filters is selected to generate the Gabor feature map.

Step 6. Feature fusion

The normalized CT image and the generated Gabor feature map are combined to obtain the enhanced representation:

$I_{\text{fused}} = \alpha I_n + (1 - \alpha)G_{\max}$

Step 7. Classification Using EfficientNetB0

The fused representation I_{fused} is supplied to the EfficientNetB0 model for binary classification:

$\hat{y} = E_\theta(I_{\text{fused}})$

$\hat{y} \in \{\text{Normal or Cancerous}\}$

Step 8. Model Evaluation

The trained model was evaluated on the independent testing set (D_{test}) testing set using six performance measures.

Step 9. Generate Grad-CAM heatmaps for explainability.

How to cite this article:
Kour P, Mansotra V (November 17, 2026) Gabor-Enhanced EfficientNet for Automated Bone Cancer Classification in Pelvic Computed Tomography (CT) Images. Cureus J Comput Sci 3 : es44389-026-00375-6. DOI https://doi.org/10.7759/s44389-026-00375-6

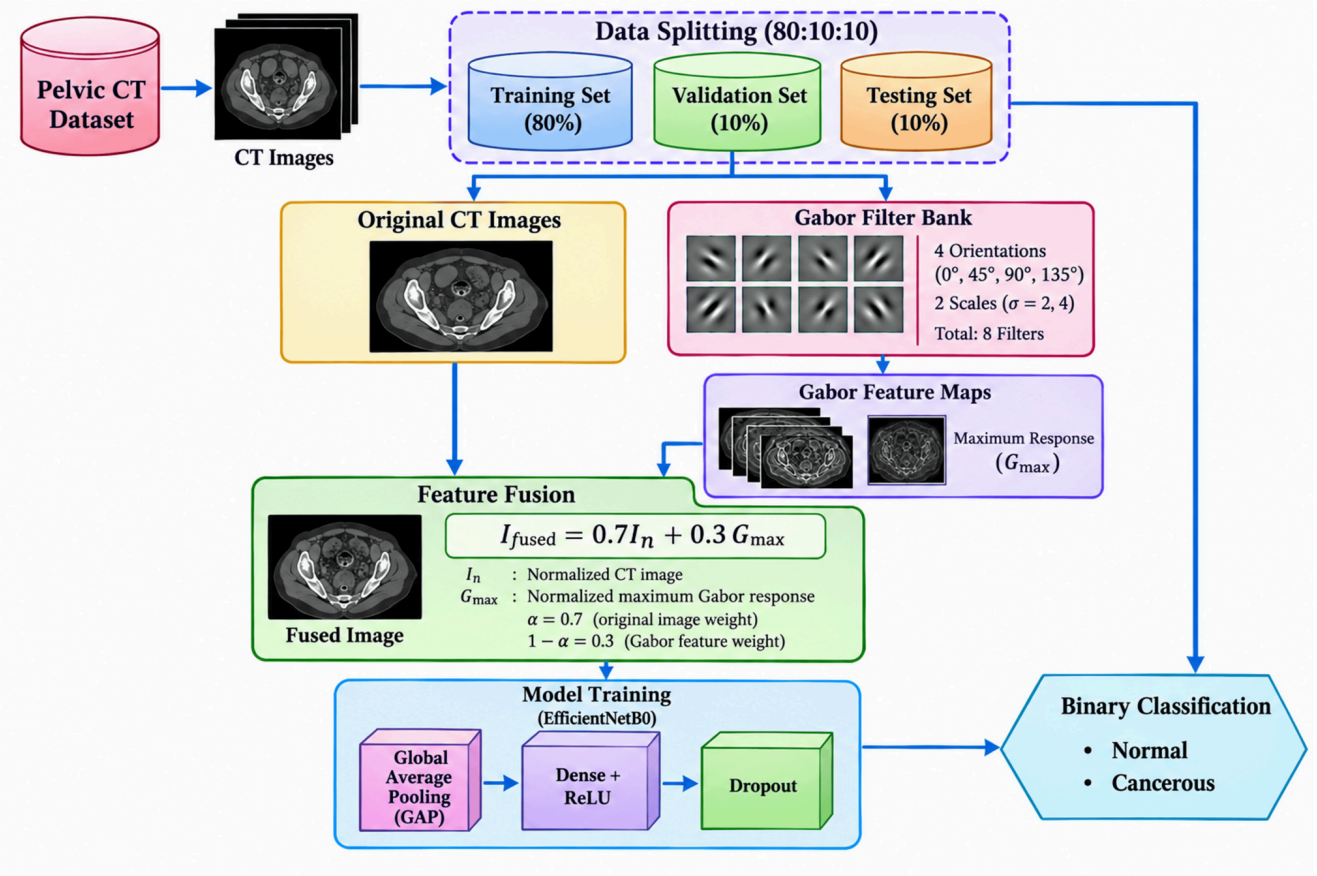


FIGURE 1: Workflow of the Gabor-Enhanced EfficientNet for bone cancer classification

CT, Computed Tomography; ReLU, Rectified Linear Unit

Dataset Description

The CT images used in this study were obtained from the publicly available Pelvic-Reference-Data collection provided through the National Cancer Institute Imaging Data Commons [19]. The collection contains pelvic CT imaging data acquired from human subjects and includes examinations involving anatomical regions such as the pelvis, prostate, and anus. The original collection was established primarily as a reference resource for pelvic image registration studies rather than specifically for bone cancer classification. To support the binary classification task, additional pelvic CT cases were obtained from multiple Radiopaedia cases, and the accompanying case descriptions were reviewed to identify examinations described as cancer-related or normal. Accordingly, the Cancerous and Normal labels in the selected dataset were assigned based on the clinical information and case descriptions available from the respective source cases.

For the present study, a subset of 732 pelvic CT images was selected for binary image classification, comprising 412 Cancerous images and 320 Normal images. The Cancerous images were selected from relevant cancer-related cases in the Pelvic-Reference-Data collection, while the Normal images were obtained from multiple Radiopaedia cases explicitly described as normal pelvic or abdominopelvic CT examinations [20]. The selected images were categorized into the Cancerous and Normal classes according to the source case descriptions and the predefined selection criteria used in this study. The resulting dataset was subsequently subjected to the specified preprocessing procedures and used for training and evaluation of the proposed deep learning model.

Data Preprocessing

After collecting the CT images from the selected datasets, it was observed that the images had different spatial resolutions and unnormalized pixel intensity values. Therefore, two preprocessing operations, namely image resizing and Min-Max normalization, were performed to obtain standardized inputs for the proposed model.

• Image Resizing: To ensure consistent input dimensions for the proposed deep learning model, all CT images were resized to a standardized resolution of 224 × 224 pixels before further processing. This standardization ensures that all images have the same dimensions before being passed to the subsequent feature extraction and classification stages.

• Min-Max Normalization: After resizing, Min-Max normalization was performed to transform the pixel intensity values into a standardized range of 0 to 1, ensuring consistent intensity scaling across all CT images. This normalization reduces variations in pixel intensity and provides a consistent input range for the subsequent Gabor texture feature extraction and EfficientNetB0 classification stages.

$$I_{\text{norm}} = \frac{I - I_{\text{min}}}{I_{\text{max}} - I_{\text{min}}}$$

where I_{norm} is the normalized pixel intensity, I denotes the original pixel intensity, and I_{min} and I_{max} correspond to the minimum and maximum pixel intensity values, respectively [21].

Data Splitting

Following preprocessing, the complete dataset was partitioned into training, validation, and testing subsets using an 80:10:10 stratified random sampling strategy. Initially, 80% of the images were allocated to the training set, while the remaining 20% were equally divided into validation and testing sets. Stratification was applied during both splitting stages to maintain a comparable distribution of the Normal and Cancerous classes across the subsets. A fixed random seed of 42 was used to ensure reproducibility. The partitioning was performed at the image level using the corresponding image paths and class labels; therefore, subject-level separation was not explicitly enforced. Consequently, images originating from the same subject may have been distributed across different subsets, which represents a potential source of subject-level information leakage and is acknowledged as a limitation of the present study.

Gabor Texture Extraction

After preprocessing, the normalized CT images were converted to grayscale and processed using a Gabor filter bank to extract relevant texture and structural information. The filter bank consisted of four orientations (0°, 45°, 90°, and 135°) and two scale parameters (σ = 2 and σ = 4), resulting in a total of eight Gabor filters [22]. A 21 × 21-pixel kernel was used for all filters. The wavelength was set to 10 pixels per cycle, the spatial aspect ratio (γ) to 0.5, and the phase offset (ψ) to 0. Each filter response was normalized to the range of 0-255, and the maximum response across all eight filters was selected to generate the final Gabor texture representation. This representation emphasizes local texture and structural variations in the CT images, which may assist in distinguishing Normal and Cancerous bone regions. The Gabor filter [23] is defined as follows:

$$G_{\text{max}}(x, y) = \max \left| G_{(s,\theta)}(x, y) \right|$$

where s and θ denote the scale and orientation of the Gabor filters, respectively, and G_{max} represents the resulting Gabor feature map.

Figure *2* shows the transformation of a preprocessed pelvic CT image using the Gabor filter. The original CT image preserved the anatomical structures of the pelvic region, while the Gabor texture image highlights local texture, edge, and directional patterns. These enhanced texture characteristics provide additional information for distinguishing bone regions.

Gabor Feature Map

The maximum response from the eight Gabor filters was selected at each pixel to generate the Gabor feature map. The response was normalized to the range of 0-255, highlighting important texture and structural patterns in the CT images. The normalized maximum Gabor response was then fused with the original CT image using a weighting scheme.

Feature Fusion

The maximum Gabor response was subsequently fused with the normalized CT image to preserve the original anatomical information while incorporating texture features. The fused image was generated by assigning a weight of 70% to the original normalized CT image and 30% to the normalized maximum Gabor response. The fusion process is defined as follows:

$$I_{\text{fused}} = \alpha I_n + (1 - \alpha) G_{\max}$$

where I_{fused} represents the fused image, I_n represents the normalized CT image, $G_{\max}$ denotes the normalized maximum Gabor response obtained by selecting the maximum response across all eight Gabor filters, and α = 0.7 controls the contribution of the original CT image, while 1 − α = 0.3 determines the contribution of the Gabor texture representation. The resulting fused image was clipped to the range of 0 to 1 and used as the input to the proposed deep learning model.

$$I_{\text{fused}} = 0.7\, I_n + 0.3\, G_{\max}$$

The feature fusion process is presented in Figure *3*. Figure *3* shows the original CT image and its corresponding Gabor texture representation. The original CT image retains the anatomical structures, whereas the Gabor representation enhances local texture and directional patterns. These complementary representations are fused to provide a richer input for the proposed Gabor-Enhanced EfficientNet model.

Classification Using EfficientNet

The fused representation I_{fused}, which integrates the structural information of the original CT image with the texture information captured by the Gabor feature map, is used as the input to the pretrained EfficientNetB0 model. The classification process can be expressed as follows:

$$\hat{y} = E_\theta(I_{\text{fused}})$$

where I_{fused} denotes the fused CT representation, E_θ represents the EfficientNetB0 classification model, and $\hat{y}$ denotes the predicted class. The model classifies the pelvic CT image into Normal or Cancerous.

$$\hat{y} \in \{\text{Normal or Cancerous}\}$$

The fused image is processed through EfficientNetB0 using an input size of 224 × 224 × 3. EfficientNetB0 was initialized with pretrained weights from the ImageNet dataset, with the original classification head removed and the backbone layers kept frozen during training. The backbone generated feature maps of size 7 × 7 × 1280, which were converted into a 1,280-dimensional feature vector using global average pooling. The resulting features were passed through a batch normalization layer and a fully connected layer containing 128 neurons with ReLU activation, followed by a dropout layer with a rate of 0.4 to reduce overfitting. Finally, a single-neuron sigmoid output layer was used for binary classification into Normal and Cancerous cases. The complete network contained 4,213,668 parameters, of which 164,097 were trainable and 4,049,571 were non-trainable. Thus, only the newly added classification layers were optimized using the pelvic CT training data, while the pretrained EfficientNetB0 backbone remained fixed.

Model Evaluation

The proposed Gabor-Enhanced EfficientNet model was evaluated using an independent test set to determine its classification performance. Six evaluation metrics, namely accuracy, precision, sensitivity, specificity, F1-score, and Matthews correlation coefficient (MCC), were considered. These metrics provide a comprehensive assessment of the

How to cite this article:
Kour P, Mansotra V (November 17, 2026) Gabor-Enhanced EfficientNet for Automated Bone Cancer Classification in Pelvic Computed Tomography (CT) Images. Cureus J Comput Sci 3 : es44389-026-00375-6. DOI https://doi.org/10.7759/s44389-026-00375-6

model's ability to distinguish between Normal and Cancerous CT images.

Explainability

To enhance the interpretability of the proposed model, Grad-CAM was employed to identify the regions of CT images that most strongly influenced the model's predictions [24]. The resulting heatmaps provide a visual representation of the areas emphasized by the Gabor-Enhanced EfficientNet during classification. This analysis helps determine whether the model attends to relevant pelvic bone regions when differentiating between Normal and Cancerous cases.

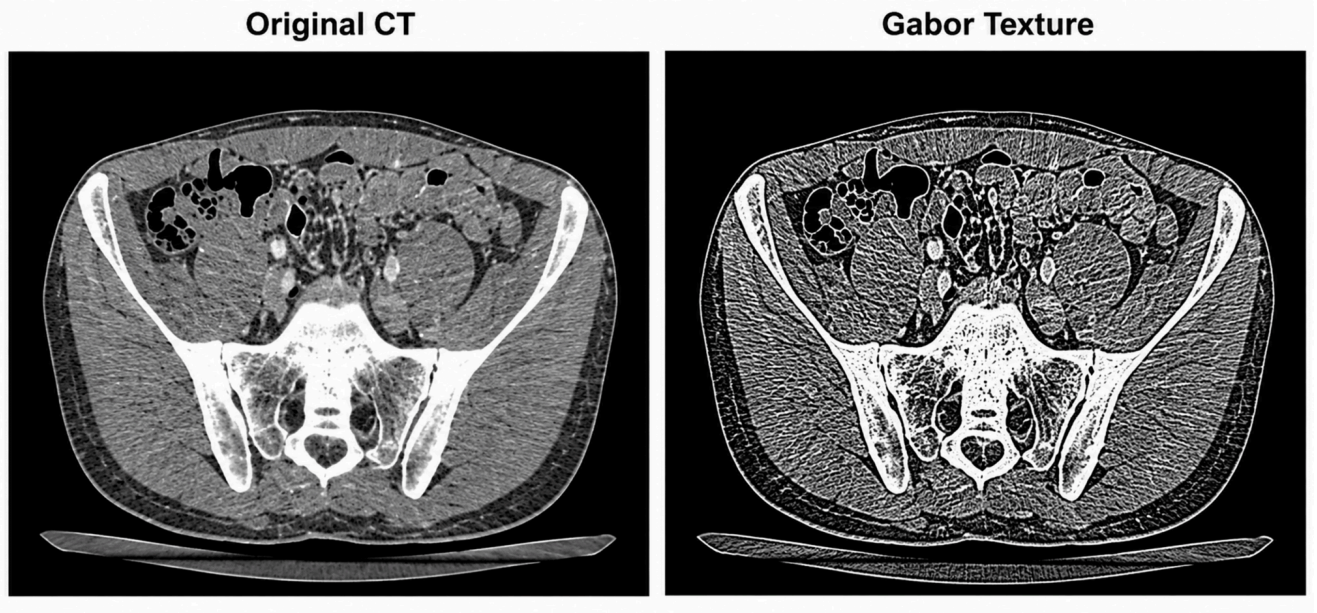


FIGURE 2: Original CT image and Gabor texture representation

CT, Computed Tomography

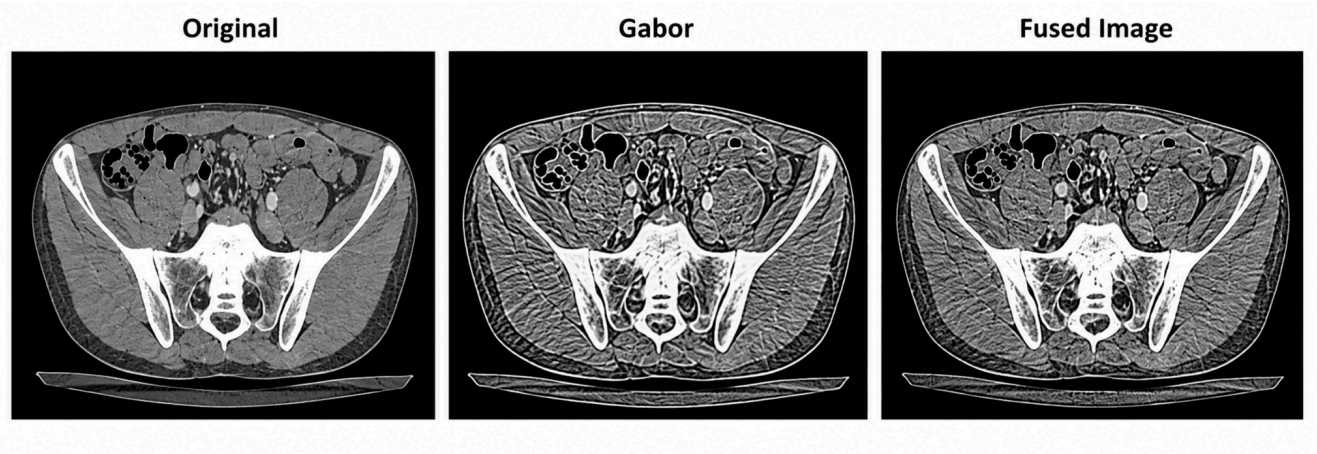


FIGURE 3: CT image transformation using feature fusion of the original CT image and Gabor texture representation

CT, Computed Tomography

How to cite this article:
Kour P, Mansotra V (November 17, 2026) Gabor-Enhanced EfficientNet for Automated Bone Cancer Classification in Pelvic Computed Tomography (CT) Images. Cureus J Comput Sci 3 : es44389-026-00375-6. DOI https://doi.org/10.7759/s44389-026-00375-6

Results And Discussion

Experimental results and analysis

This section outlines the experimental setup of the proposed Gabor-Enhanced EfficientNet model and describes the evaluation measures used to assess its performance. The model is evaluated for the binary classification of pelvic CT images into Normal and Cancerous categories.

Experimental Setup

The proposed Gabor-Enhanced EfficientNet framework was developed and implemented in a Google Colab environment using the required Python libraries and a GPU-based computing environment to accelerate model training. The pelvic CT dataset was partitioned into training, validation, and testing subsets in an 80:10:10 ratio, respectively. The proposed model was trained for up to 30 epochs using a batch size of 16. An early stopping strategy was employed by monitoring the validation loss (val_loss). Training was stopped when the validation loss did not improve for six consecutive epochs, and the model weights corresponding to the lowest validation loss were restored. This approach helped reduce overfitting and unnecessary computational effort.

Hyperparameter Tuning

The key hyperparameters used for the proposed EfficientNetB0 model are presented in Table 2. The model used 224 × 224 × 3 input images, a batch size of 16, and 30 initial training epochs. Fine-tuning was performed for 10 additional epochs using a reduced learning rate of 1×10^{-5}. The Adam optimizer and binary cross-entropy loss were used for classification.

Hyperparameter	Value
Input image size	224 × 224 × 3
Pre-trained weights	ImageNet
Batch size	16
Initial training epochs	30
Initial learning rate	1×10^{-4}
Fine-tuning epochs	10
Fine-tuning learning rate	1×10^{-5}
Trainable layers during fine-tuning	Last 30 layers
Dense layer	256 units, rectified linear unit
Dropout rate	0.3
Optimizer	Adam
Loss function	Binary cross-entropy

How to cite this article:
Kour P, Mansotra V (November 17, 2026) Gabor-Enhanced EfficientNet for Automated Bone Cancer Classification in Pelvic Computed Tomography (CT) Images. Cureus J Comput Sci 3 : es44389-026-00375-6. DOI https://doi.org/10.7759/s44389-026-00375-6

Output activation	Sigmoid
Random seed	42

TABLE 2: Key hyperparameters of the proposed Gabor-Enhanced EfficientNet for bone cancer classification

Performance Analysis

The classification performance of the proposed model was evaluated using standard metrics derived from the confusion matrix presented in Figure *4*. The test set contained 74 CT images, of which 29 Normal images were correctly classified as Normal (true negative) and 42 Cancerous images were correctly classified as Cancerous (true positive). In addition, 3 Normal images were incorrectly classified as Cancerous (false positive), while no Cancerous images were misclassified as Normal (false negative = 0).

The classification performance of the proposed Gabor-Enhanced EfficientNet model is presented in Table *3*. Based on the reported results, the model achieved an accuracy of 95.95%, demonstrating strong overall classification performance. It obtained a precision of 93.33% and a sensitivity of 100.00%, indicating that all Cancerous cases were correctly identified. The specificity of 90.63% indicates that the model also effectively distinguished Normal cases. Furthermore, the F1-score of 96.55% demonstrates a favorable balance between precision and sensitivity, while the MCC of 0.9197 indicates strong agreement between the predicted and actual class labels. Overall, these results demonstrate that the proposed Gabor-Enhanced EfficientNet model provides effective classification of Normal and Cancerous pelvic CT images.

Performance Curves

To provide a more comprehensive assessment of the proposed Gabor-Enhanced EfficientNet model, the ROC curve, training and validation accuracy curves, and training and validation loss curves were examined.

Figure *5* shows the training and validation accuracy of the proposed model over successive epochs. The training accuracy increases from approximately 58% in the first epoch to 88.5% in the final epoch, while the validation accuracy improves from approximately 56% to 86.5%. Both curves exhibit a gradual upward trend throughout training, indicating progressive learning of discriminative features from the pelvic CT images. The relatively close trends of the training and validation curves, with no substantial divergence, indicate stable model learning and reasonably consistent validation performance.

Figure *6* presents the training and validation loss of the proposed model across successive epochs. Both loss curves exhibit a consistent downward trend, indicating progressive improvement and convergence during training. The training loss decreased from approximately 0.73 in the first epoch to 0.54 in the final epoch, while the validation loss decreased from approximately 0.70 to 0.55. The close alignment and similar decreasing trends of the two curves indicate stable convergence, with no substantial divergence between training and validation loss during the training process.

Furthermore, Figure *7* illustrates the ROC curve, demonstrating the ability of the proposed model to distinguish between Normal and Cancerous pelvic CT images across different classification thresholds. The ROC curve remains close to the upper-left corner, indicating a high true-positive rate with a low false-positive rate. The model achieved an area under the curve (AUC) of 0.9963, demonstrating excellent discriminative performance in distinguishing between Cancerous and Normal cases.

Taken together, Figures *5*-*7* demonstrate the learning behavior and classification performance of the proposed pelvic CT classification framework. The training and validation accuracy and loss curves show gradual convergence with no pronounced divergence between the training and validation trends, indicating stable model learning and reasonably consistent validation performance. The ROC curve further demonstrates excellent discriminative ability, with an AUC of 0.9963, indicating that the model effectively distinguishes between Normal and Cancerous pelvic CT images.

Explainability

Grad-CAM was employed to interpret the predictions of the proposed Gabor-Enhanced model by identifying the image regions that contributed most to its classification decisions. The input CT image was first processed using Gabor filters to capture relevant directional textures and structural patterns. The enhanced Gabor representation was then fused with the original CT image and provided to the classification network. The resulting Grad-CAM heatmap identifies the regions that contributed most to the Cancerous prediction, as shown in Figure *8*. The highlighted areas are mainly concentrated around the pelvic bone and surrounding anatomical structures, indicating that the model focuses on relevant structural and textural characteristics. This visualization demonstrates that the proposed model bases its prediction on meaningful regions of the CT image, thereby improving the interpretability of the classification process [25].

Ablation Study

An ablation study was conducted to investigate the effect of different CT-Gabor texture fusion ratios on classification performance. Three fusion configurations were evaluated: 80% CT + 20% Gabor texture, 70% CT + 30% Gabor texture, and 60% CT + 40% Gabor texture. Accuracy, precision, sensitivity, specificity, F1-score, and MCC, together with their corresponding 95% confidence intervals, were calculated for each configuration. The complete performance results are presented in Table *3*. Among the evaluated configurations, the 70% CT + 30% Gabor texture fusion achieved the highest overall performance across the primary classification metrics, indicating that this fusion ratio provided a favorable balance between the original CT information and the extracted Gabor texture features.

Comparison

As only a limited number of studies have specifically addressed CT-based bone cancer classification, Table *4* compares the proposed framework with the available relevant studies. Jagadeesh and Kumar [26] reported 79.9% accuracy using an Enhanced Residual Network for porous (cancerous) versus normal bone classification from CT scans. A 2023 deep learning-based framework reported 77% accuracy, 79% sensitivity, and 75% specificity for benign versus malignant bone tumor classification using femur CT images. In comparison, the proposed Gabor texture-enhanced CT fusion with EfficientNetB0 achieved 95.95% accuracy, 93.33% precision, 100% sensitivity, 90.63% specificity, 96.55% F1-score, 0.9197 MCC, and 0.9963 AUC for Normal versus Cancerous pelvic CT classification. These results demonstrate strong performance on the evaluated pelvic CT dataset.

How to cite this article:
Kour P, Mansotra V (November 17, 2026) Gabor-Enhanced EfficientNet for Automated Bone Cancer Classification in Pelvic Computed Tomography (CT) Images. Cureus J Comput Sci 3 : es44389-026-00375-6. DOI https://doi.org/10.7759/s44389-026-00375-6

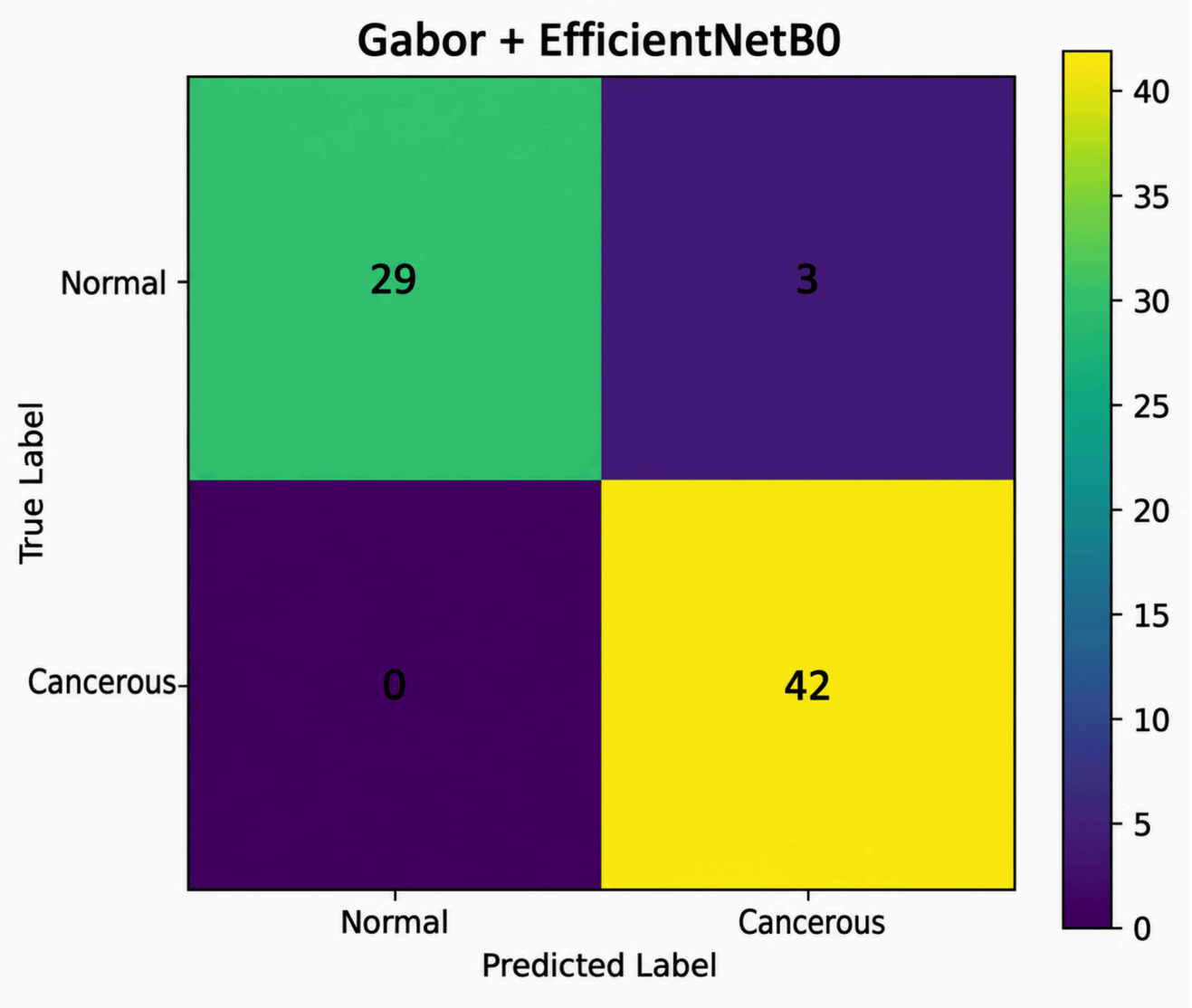


FIGURE 4: Confusion matrix for the Gabor-Enhanced EfficientNet model for bone cancer classification

Metric	80% CT + 20% Gabor texture		70% CT + 30% Gabor texture		60% CT + 40% Gabor texture	
	Result	95% CI	Result	95% CI	Result	95% CI
Accuracy	93.18%	87.50–97.73%	95.95%	88.7–98.6%	78.77%	71.44–84.62%
Precision	89.29%	80.39–96.55%	93.33%	82.1–97.7%	83.12%	73.23–89.86%
Sensitivity	100%	97.86–100%	100.00%	91.6–100%	78.05%	67.95–85.64%
Specificity	84.21%	70.58–94.74%	90.63%	75.8–96.8%	79.69%	68.29–87.73%
F1-Score	94.34%	89.13–98.25%	96.55%	91.95–100%	80.50%	75.0–84.8%

How to cite this article:
Kour P, Mansotra V (November 17, 2026) Gabor-Enhanced EfficientNet for Automated Bone Cancer Classification in Pelvic Computed Tomography (CT) Images. Cureus J Comput Sci 3 : es44389-026-00375-6. DOI https://doi.org/10.7759/s44389-026-00375-6

MCC	0.8671	0.760–0.954%	0.9197	0.825–100	0.574	0.44–0.60

TABLE 3: Classification performance of the Gabor-Enhanced EfficientNet model for bone cancer classification

CT, Computed Tomography; MCC, Matthews Correlation Coefficient

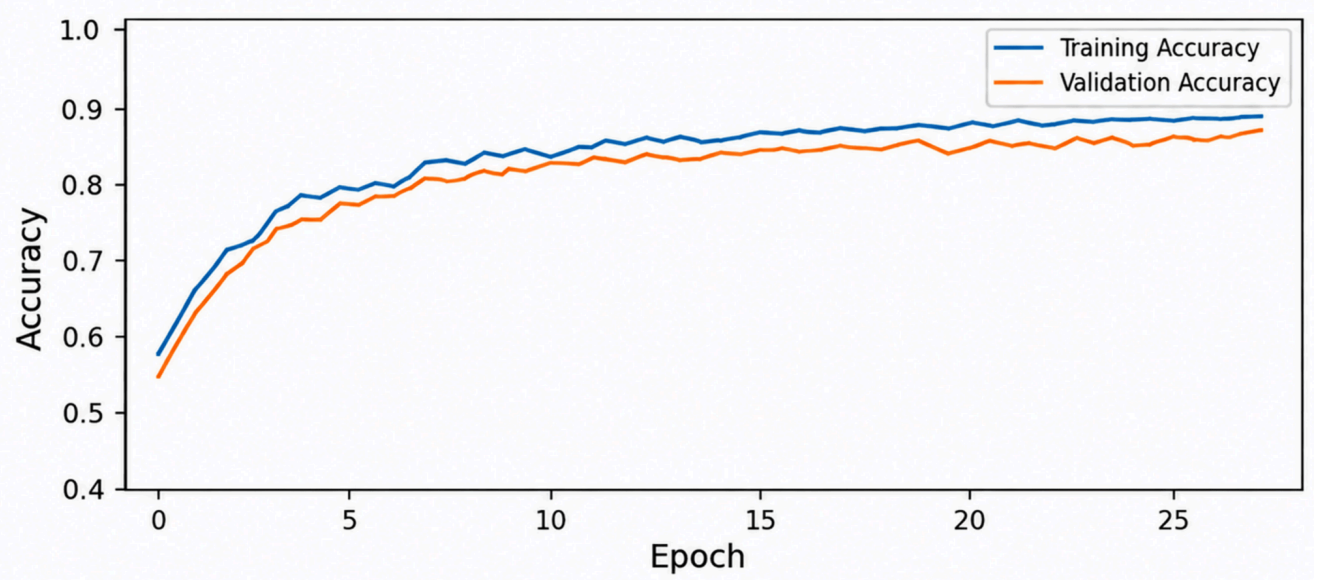


FIGURE 5: Accuracy curves of the Gabor-Enhanced EfficientNet model for pelvic CT bone cancer classification

CT, Computed Tomography

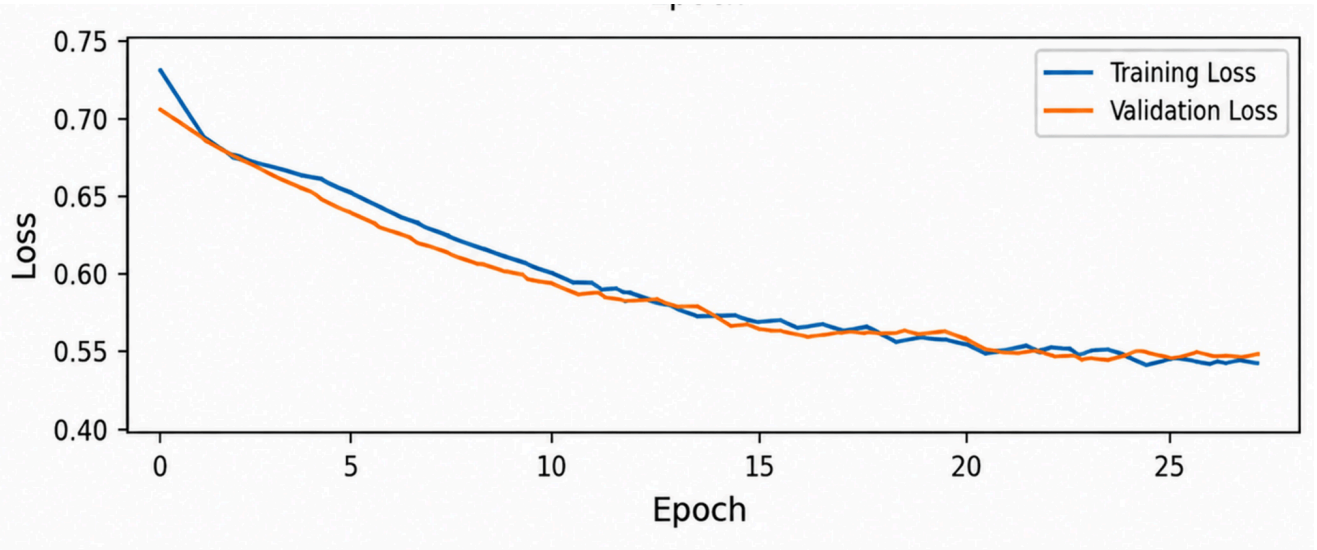


FIGURE 6: Loss curves of the Gabor-Enhanced EfficientNet model for pelvic CT bone cancer classification

CT, Computed Tomography

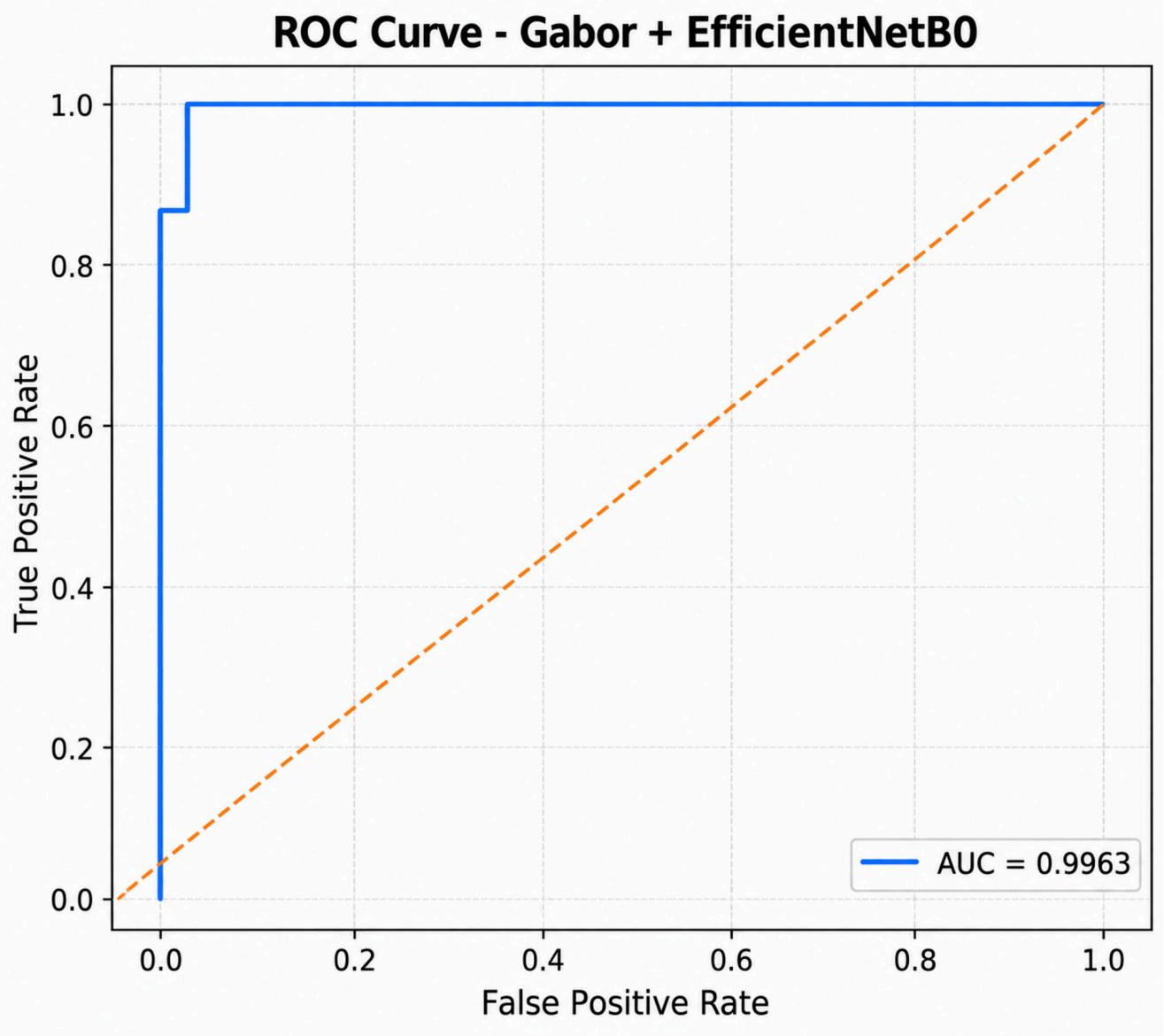


FIGURE 7: ROC curve of the Gabor-Enhanced EfficientNet for pelvic CT bone cancer classification

AUC, Area Under the Curve; CT, Computed Tomography; ROC, Receiver Operating Characteristic

How to cite this article:
Kour P, Mansotra V (November 17, 2026) Gabor-Enhanced EfficientNet for Automated Bone Cancer Classification in Pelvic Computed Tomography (CT) Images. Cureus J Comput Sci 3 : es44389-026-00375-6. DOI https://doi.org/10.7759/s44389-026-00375-6

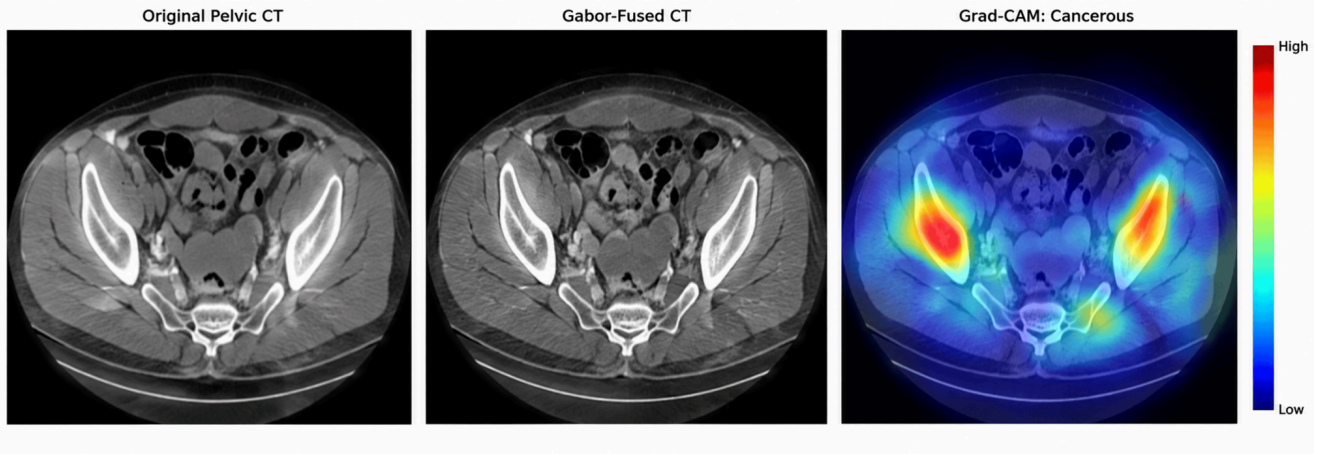


FIGURE 8: Grad-CAM visualization of the proposed Gabor-Enhanced EfficientNet model for cancer prediction

CT, Computed Tomography; Grad-CAM, Gradient-weighted Class Activation Mapping

Reference	Method/Architecture	Imaging Modality	Classification Task	Reported Performance
Jagadeesh and Kumar [26]	Enhanced Residual Network	CT scan	Porous (Cancerous) bone vs. Normal bone	Accuracy: 79.9%
Potter et al. [7] (Automated Bone Tumor Segmentation and Classification)	Deep learning-based segmentation and classification framework	Femur CT	Benign vs. Malignant bone tumors	Accuracy: 77%; Sensitivity: 79%; Specificity: 75%
Proposed Method	Gabor texture-enhanced CT fusion + EfficientNet-B0	Pelvic CT	Normal vs. Cancerous	Accuracy: 95.95%; Precision: 93.33%; Sensitivity: 100%; Specificity: 90.63%; F1-score: 96.55%; MCC: 0.9197; AUC: 0.9963

TABLE 4: Comparison of the proposed framework with existing CT-based bone cancer classification methods

AUC, Area Under the Curve; CT, Computed Tomography; MCC, Matthews Correlation Coefficient

Conclusions

The proposed Gabor-Enhanced EfficientNet model was developed for automated bone cancer classification using CT images. The images were preprocessed to obtain standardized inputs, followed by Gabor filtering to capture relevant texture, edge, and directional patterns. The Gabor representation was fused with the original CT image, enabling the model to utilize both anatomical and texture information. The fused input was then processed by EfficientNet to classify images into Normal and Cancerous categories. Despite the promising classification performance, the study has some limitations. The dataset was derived from limited source collections, and the Cancerous and Normal labels were assigned based on the clinical descriptions available with the source cases rather than independent clinical or pathological

How to cite this article:
Kour P, Mansotra V (November 17, 2026) Gabor-Enhanced EfficientNet for Automated Bone Cancer Classification in Pelvic Computed Tomography (CT) Images. Cureus J Comput Sci 3 : es44389-026-00375-6. DOI https://doi.org/10.7759/s44389-026-00375-6

confirmation. In addition, the current framework performs 2D image-level classification and may not fully capture the three-dimensional characteristics of CT volumes. Therefore, the results should be interpreted as an initial evaluation rather than definitive clinical validation.

In future work, the proposed model will be evaluated using larger, multi-center CT datasets with independently verified clinical labels and patient-wise data splitting to reduce potential data leakage and improve the assessment of model generalizability and clinical reliability. The framework can also be extended to three-dimensional CT analysis and multi-class bone cancer classification to enable more comprehensive disease characterization.

Additional Information

Author Contributions

All authors have reviewed the final version to be published and agreed to be accountable for all aspects of the work.

Concept and design: Paramjit Kour, Vibhakar Mansotra

Acquisition, analysis, or interpretation of data: Paramjit Kour

Drafting of the manuscript: Paramjit Kour, Vibhakar Mansotra

Critical review of the manuscript for important intellectual content: Paramjit Kour, Vibhakar Mansotra

Supervision: Paramjit Kour, Vibhakar Mansotra

Disclosures

Human subjects: All authors have confirmed that this study did not involve human participants or tissue.

Animal subjects: All authors have confirmed that this study did not involve animal subjects or tissue.

Conflicts of interest: In compliance with the ICMJE uniform disclosure form, all authors declare the following:

- **Payment/services info:** All authors have declared that no financial support was received from any organization for the submitted work.
- **Financial relationships:** All authors have declared that they have no financial relationships at present or within the previous three years with any organizations that might have an interest in the submitted work.
- **Other relationships:** All authors have declared that there are no other relationships or activities that could appear to have influenced the submitted work.

Data Availability Statements

The data (and/or code) supporting this study are openly available in National Institute Cancer Imaging Data Commons at https://portal.imaging.datacommons.cancer.gov/explore/, reference Pelvic-Reference-Data.

References

1. Xu H, Zhao Q, Miao X, Zhu L, Wang J: Clinical decision-making in bone cancer care management and forecast of ICU needs based on computed tomography. Journal of Bone Oncology. 2024, 49:100646. 10.1016/j.jbo.2024.100646

2. Jung H: Basic physical principles and clinical applications of computed tomography. Progress in Medical Physics. 2021, 32:1-17. 10.14316/pmp.2021.32.1.1

3. Zhao X, Dong Y, Xu L, Shen Y, Qin G, Zhang Z: Deep bone oncology diagnostics: Computed tomography based machine learning for detection of bone tumors from breast cancer metastasis. Journal of Bone Oncology. 2024, 48:100638. 10.1016/j.jbo.2024.100638

How to cite this article:
Kour P, Mansotra V (November 17, 2026) Gabor-Enhanced EfficientNet for Automated Bone Cancer Classification in Pelvic Computed Tomography (CT) Images. Cureus J Comput Sci 3 : es44389-026-00375-6. DOI https://doi.org/10.7759/s44389-026-00375-6

4. Ahlawat S, Lenchik L, Baker JC, et al.: ACR Appropriateness Criteria® suspected primary bone tumors: 2024 update. Journal of the American College of Radiology. 2025, 22:440-454. 10.1016/j.jacr.2025.02.020

5. Zhang P, Yang Z: Convolutional neural networks: Applications, challenges and future prospects in brain tumor research. Frontiers in Neurology. 2026, 17:1759459. 10.3389/fneur.2026.1759459

6. Ali I, Manda VK: Artificial intelligence for predicting progression and personalizing healthcare to Alzheimer's disease patients. AI-Driven Personalized Healthcare Solutions. Chemingui H (ed): IGI Global Scientific Publishing, Hershey, PA; 2025. 155-190. 10.4018/979-8-3693-7858-8.ch006

7. Potter IY, Yeritsyan D, Mahar S, Wu J, Nazarian A, Vaziri A: Automated bone tumor segmentation and classification as benign or malignant using computed tomographic imaging. Journal of Imaging Informatics in Medicine. 2023, 36:869-878. 10.1007/s10278-022-00771-z

8. Deivasigamani S, Senthilpari C, D SSR, Thankaraj A, Narmadha G, Gowrishankar K: Gabor transform-based deep learning system using CNN for melanoma detection. Computers. 2026, 15:54. 10.3390/computers15010054

9. Cai J, Liu M, Zhang Q, et al.: Renal cancer detection: Fusing deep and texture features from histopathology images. BioMed Research International. 2022, 2022:9821773. 10.1155/2022/9821773

10. Karim AHMZ, Mahmud KBO, Shahnaz C: A hybrid feature extraction based ensemble model for breast cancer detection and classification using different medical images. Intelligence-Based Medicine. 2025, 12:100290. 10.1016/j.ibmed.2025.100290

11. Attallah O: Skin cancer classification leveraging multi-directional compact convolutional neural network ensembles and Gabor wavelets. Scientific Reports. 2024, 14:20637. 10.1038/s41598-024-69954-8

12. Sarvestani ZM, Jamali J, Taghizadeh M, Dindarloo MHF: A novel machine learning approach on texture analysis for automatic breast microcalcification diagnosis classification of mammogram images. Journal of Cancer Research and Clinical Oncology. 2023, 149:6151-6170. 10.1007/s00432-023-04571-y

13. Kour P, Mansotra V: GCNN: A convolutional neural network with Gabor filter for the classification of pelvic bone cancer MRI images. Modern Practices and Trends in Expert Applications and Security. MP-TEAS 2024. Rathore VS, Murala S, Tuba E, Singh MM (ed): Springer, Singapore; 2025. 1379:71-83. 10.1007/978-981-96-5784-1_7

14. Bakheet S, Al-Hamadi A: Computer-aided diagnosis of malignant melanoma using Gabor-based entropic features and multilevel neural networks. Diagnostics. 2020, 10:822. 10.3390/diagnostics10100822

15. Al-Kadi OS: A Gabor filter texture analysis approach for histopathological brain tumor subtype discrimination [PREPRINT]. arXiv. 2017, 10.48550/arXiv.1704.05122

16. Linder N, Konsti J, Turkki R, et al.: Identification of tumor epithelium and stroma in tissue microarrays using texture analysis. Diagnostic Pathology. 2012, 7:22. 10.1186/1746-1596-7-22

17. Kumar V, Chandrashekhara KT, Jagini NP, Rajkumar KV, Godi RK, Tumuluru P: Enhanced breast cancer detection and classification via CAMR-Gabor filters and LSTM: A deep Learning-Based method. Egyptian Informatics Journal. 2025, 29:100602. 10.1016/j.eij.2024.100602

18. Santiago-Montero R, Calzada-Ledesma V, Gutiérrez-Hernández DA, Ortiz-Aguilar LdM, Mares-Castro A, Xoca-Orozco LA, Flores-Sierra JdJ: Evolutionarily optimized multi-scale Gabor modeling of directional lesion texture in dermoscopic images for interpretable melanoma classification. Diagnostics. 2026, 16:1430. 10.3390/diagnostics16101430

19. NCI Imaging Data Commons. (2026). Accessed: July 23, 2026: https://portal.imaging.datacommons.cancer.gov/explore/.

20. Caes. Radiopaedia.org. (2026). Accessed: September 23, 2026: https://radiopaedia.org/search?scope=cases&sort=date_of_publication.

21. Henderi H, Wahyuningsih T, Rahwanto E: Comparison of min-max normalization and z-score normalization in the k-nearest neighbor (kNN) algorithm to test the accuracy of types of breast cancer. International Journal of Informatics and Information Systems. 2021, 4:13-20. 10.47738/ijiis.v4i1.73

22. Han F, Wang H, Zhang G, et al.: Texture feature analysis for computer-aided diagnosis on pulmonary nodules. Journal of Imaging Informatics in Medicine. 2015, 28:99-115. 10.1007/s10278-014-9718-8

23. Dakshayani V, Locharla GR, Pławiak P, Datti V, Karri C: Design of a Gabor filter-based image denoising hardware model. Electronics. 2022, 11:1063. 10.3390/electronics11071063

How to cite this article:
Kour P, Mansotra V (November 17, 2026) Gabor-Enhanced EfficientNet for Automated Bone Cancer Classification in Pelvic Computed Tomography (CT) Images. Cureus J Comput Sci 3 : es44389-026-00375-6. DOI https://doi.org/10.7759/s44389-026-00375-6

24. Selvaraju RR, Cogswell M, Das A, Vedantam R, Parikh D, Batra D: Grad-CAM: Visual explanations from deep networks via gradient-based localization. International Journal of Computer Vision. 2020, 128:336-359. 10.1007/s11263-019-01228-7

25. Christy V, Manda VK, Gnanadasan ML: Ethical frameworks for use in artificial intelligence systems. Generative AI and Implications for Ethics, Security, and Data Management. Sankar JG, David A (ed): IGI Global Scientific Publishing, Hershey, PA; 2024. 122-154. 10.4018/979-8-3693-8557-9.ch005

26. Jagadeesh A, Kumar S: Identifying the porous bones in CT scan dataset bone using enhanced residual network over traditional convolutional neural network. Journal of Pharmaceutical Negative Results. 2022, 13:1592-1601. 10.47750/pnr.2022.13.S04.190

How to cite this article:
Kour P, Mansotra V (November 17, 2026) Gabor-Enhanced EfficientNet for Automated Bone Cancer Classification in Pelvic Computed Tomography (CT) Images. Cureus J Comput Sci 3 : es44389-026-00375-6. DOI https://doi.org/10.7759/s44389-026-00375-6